

# Enhancement of acoustic sensitivity of hollow-core photonic bandgap fibers

Fan Yang,<sup>1</sup> Wei Jin,<sup>1,\*</sup> Hoi Lut Ho,<sup>1</sup> Fuyin Wang,<sup>2</sup> Wen Liu,<sup>2</sup> Lina Ma,<sup>2</sup> and Yongming Hu<sup>2</sup>

<sup>1</sup> Department of Electrical Engineering, The Hong Kong Polytechnic University, Hong Kong, China

<sup>2</sup> College of Opto-Electro Science and Engineering, National University of Defense Technology, Changsha, 410073, China

\*ewjin@polyu.edu.hk

**Abstract:** The acoustic pressure sensitivities of hollow-core photonic bandgap fibers (HC-PBFs) with different thicknesses of silica outer-cladding and polymer jacket were experimentally investigated. Experiment with a HC-PBF with 7  $\mu\text{m}$ -thick silica outer cladding and 100  $\mu\text{m}$ -thick Parylene C jacket demonstrated a pressure sensitivity 10 dB higher than the commercial HC-1550-02 fiber and 25 dB higher than a standard single mode fiber. The significant enhancement in sensitivity would simplify the design of fiber hydrophone arrays and increase the number of sensors that could be multiplexed in a single fiber.

©2013 Optical Society of America

**OCIS codes:** (060.2370) Fiber optics sensors; (060.5295) Photonic crystal fibers; (120.5050) Phase measurement; (120.5475) Pressure measurement.

---

## References and links

1. J. A. Bucaro, H. D. Dardy, and E. F. Carome, "Fiber optic hydrophone," *J. Acoust. Soc. Am.* **62**(5), 1302–1304 (1977).
2. J. H. Cole, R. L. Johnson, and P. G. Bhuta, "Fiber optic detection of sound," *J. Acoust. Soc. Am.* **62**(5), 1136–1138 (1977).
3. B. Budiansky, D. C. Drucker, G. S. Kino, and J. R. Rice, "Pressure sensitivity of a clad optical fiber," *Appl. Opt.* **18**(24), 4085–4088 (1979).
4. R. Hughes and J. Jarzynski, "Static pressure sensitivity amplification in interferometric fiber-optic hydrophones," *Appl. Opt.* **19**(1), 98–107 (1980).
5. N. Lagakos, E. U. Schnaus, J. H. Cole, J. Jarzynski, and J. A. Bucaro, "Optimizing fiber coatings for interferometric acoustic sensors," *IEEE J. Quantum Electron.* **18**(4), 683–689 (1982).
6. J. A. Bucaro, N. Lagakos, H. H. Cole, and T. G. Giallorenzi, "Fiber optic acoustic transduction," in *Physical Acoustics vol 16*, W. P. Mason and R. N. Thurston, eds. (Academic Press Inc, 1982), pp. 385–457.
7. G. McDearmon, "Theoretical analysis of a push-pull fiber-optic hydrophone," *J. Lightwave Technol.* **5**(5), 647–652 (1987).
8. C. K. Kirkendall and A. Dandridge, "Overview of high performance fiber-optic sensing," *J. Phys. D* **37**(18), 197–216 (2004).
9. J. H. Cole, C. Sunderman, A. B. Tveten, C. Kirkendall, and A. Dandridge, "Preliminary investigation of air-included polymer coatings for enhanced sensitivity of fiber-optic acoustic sensors," in *Proceedings of 15th International Conference on Optical Fiber Sensors* (Portland, 2002), pp. 317–320.
10. J. H. Cole, S. Mothley, J. Jarzynski, A. B. Tveten, C. Kirkendall, and A. Dandridge, "Air-included polymer coatings for enhanced sensitivity of fiber-optic acoustic sensors," in *Proceedings of 16th International Conference on Optical Fiber Sensors*, (Nara, 2003), pp. 214–217.
11. M. Pang and W. Jin, "Detection of acoustic pressure with hollow-core photonic bandgap fiber," *Opt. Express* **17**(13), 11088–11097 (2009).
12. M. Pang, H. F. Xuan, J. Ju, and W. Jin, "Influence of strain and pressure to the effective refractive index of the fundamental mode of hollow-core photonic bandgap fibers," *Opt. Express* **18**(13), 14041–14055 (2010).
13. Specialty Coating Systems website, <http://scscoatings.com>
14. T. A. Harder, T. J. Yao, Q. He, C. Y. Shih, and Y. C. Tai, "Residual stress in thin-film parylene-C," in *Proceedings of IEEE Conference on Micro Electro Mechanical Systems* (Las Vegas, 2002), pp. 435–438.
15. A. D. Kersey, M. J. Marrone, and M. A. Davis, "Polarisation-insensitive fibre optic Michelson interferometer," *Electron. Lett.* **27**(6), 518–520 (1991).
16. Y. M. Hu, Z. L. Hu, H. Luo, and L. N. Ma, "Recent progress toward fiber optic hydrophone research, application and commercialization in China," *Proc. SPIE* **8421**, 22nd International Conference on Optical Fiber Sensors, 84210Q (2012).

17. A. Dandridge, A. B. Tveten, and T. G. Giallorenzi, "Homodyne demodulation scheme for fiber optic sensors using phase generated carrier," *IEEE Trans. Microw. Theory Tech.* **30**(10), 1635–1641 (1982).
  18. L. J. Gibson and M. F. Ashby, *Cellular Solids: Structure and Properties II* (Cambridge University, 1997), Chap. 4.
  19. R. M. Christensen, "Mechanics of cellular and other low-density materials," *Int. J. Solids Struct.* **37**(1-2), 93–104 (2000).
  20. V. Dangui, H. K. Kim, M. Digonnet, and G. Kino, "Phase sensitivity to temperature of the fundamental mode in air-guiding photonic-bandgap fibers," *Opt. Express* **13**(18), 6669–6684 (2005).
  21. Shared Materials Instruction Facility in Duke University, <https://smif.lab.duke.edu/pdf/UsefulParametersForParyleneDeposition.pdf>
  22. Y. Liu and M. B. Huglin, "Effective crosslinking densities and elastic moduli of some physically crosslinked hydrogels," *Polymer (Guildf.)* **36**(8), 1715–1718 (1995).
  23. J. M. Williams, J. J. Bartos III, and M. H. Wilkerson, "Elastic modulus dependence on density for polymeric foams with systematically changing microstructures," *J. Mater. Sci.* **25**(12), 5134–5141 (1990).
- 

## 1. Introduction

The first interferometric fiber hydrophones were demonstrated in 1970s [1, 2]. In the early time, bare optical fiber was used and the pressure sensitivity in terms of normalized responsivity (NR), defined as the phase change per unit change of acoustic pressure normalized to the total phase shift, was very low. The pressure sensitivity was improved by coating the fiber with a material of a lower bulk modulus [3–5]. NR was significantly increased by wrapping the fiber around a properly designed air-backed plastic mandrel [6, 7]. The mandrel-based hydrophones have demonstrated sufficient NR and satisfied the need of some practical applications. However, the costs of the mandrel-based systems are high especially for large scale multiplexed sensor arrays [8].

An alternative is to coat the fiber directly with an appropriate polymeric material to increase its NR. A short silica fiber coated with thick air-included polymer (~8 mm in diameter including the silica fiber) has demonstrated a similar NR to the mandrel-based hydrophones [9, 10].

Compared with conventional solid single mode fibers (SMFs), the phase sensitivity of the fundamental mode to pressure in a hollow-core photonic bandgap fiber (HC-PBF) is anticipated to be significantly higher [11]. This is because that there are many air columns along the fiber, which significantly reduce the effective Young's modulus and increase the axial strain due to acoustic pressure. In addition, the fundamental mode travels mostly in air as opposed to silica in conventional SMF, and hence the refractive index change due to acoustic pressure, which compromises the phase sensitivity in conventional SMF, is also reduced [12]. Experiment with a commercial HC-PBF (HC-1550-02 from NKT Photonics) demonstrated a NR ~15 dB higher than a conventional SMF [11], and the NR could be further enhanced by reducing the thickness of the outer silica cladding and coating the fiber with an appropriate elastic polymer.

In this paper, we demonstrate experimentally the improvement of pressure sensitivity by another 10 dB by thinning of the silica cladding by chemical etching and then re-coating of the fiber with a special polymer, demonstrating the potential of an optimized HC-PBF for high sensitivity acoustic detection.

## 2. Fabrication of HC-PBF samples for acoustic sensing

The HC-PBF samples were derived from the commercial HC-1550-02 fiber (Fig. 1(a)) by etching away part of its silica outer cladding and re-coating it with a soft polymer jacket. A section of HC-1550-02 fiber (37 cm in length) was firstly spliced to SMFs at both ends, and hydrofluoric acid (Honeywell, 49% HF in H<sub>2</sub>O by weight) was then used to etch away part of the outer silica cladding. The etching was carried out at room temperature (~25 °C) and the etching rate is ~1.3 μm/min. Figure 1(b) shows the cross-section of HC-PBF after ~9 min etching, the thickness of the outer silica cladding is estimated to be ~13 μm.

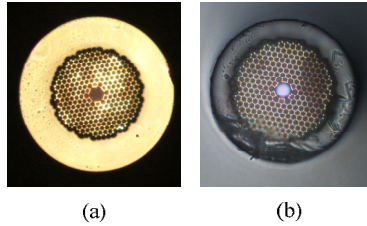


Fig. 1. Cross-section of HC-1550-02 fiber. Core diameter: 10.9  $\mu\text{m}$ , inner microstructured cladding diameter: 70  $\mu\text{m}$ . (a) Before etching by HF acid, the outer cladding diameter is 120  $\mu\text{m}$ , and (b) after 9 min etching by HF acid, the outer cladding diameter is 96  $\mu\text{m}$ .

The etched fiber was then coated with Parylene C by a special chemical vapor deposition system, which has uniform coating quality, controllable coating thickness and deposition rate [13]. With this system, long fibers with a length of tens of centimeters can be coated with a polymer jacket with a desirable thickness. The deposition process begins with the granular form of Parylene C (raw material dimmer). The material is vaporized under vacuum and heated to a dimeric gas. The gas is then pyrolyzed to cleave the dimer to its monomeric form. In a room temperature deposition chamber, the monomer gas deposits on the surface of the fiber as a transparent polymer film. By controlling the evaporation time, coating thickness from hundreds of angstroms to a few hundreds of microns could be obtained. Under deposition pressure 25 mTorr, the Young's modulus and Poisson's ratio of Parylene C are quoted to be 2.758 GPa and 0.4, respectively [13, 14].

Figure 2(a) shows the fixture of the fiber within the deposition chamber, and the cross-section of a HC-PBF sample coated with Parylene C to an outer diameter of  $\sim 284$   $\mu\text{m}$  is shown in Fig. 2(b).

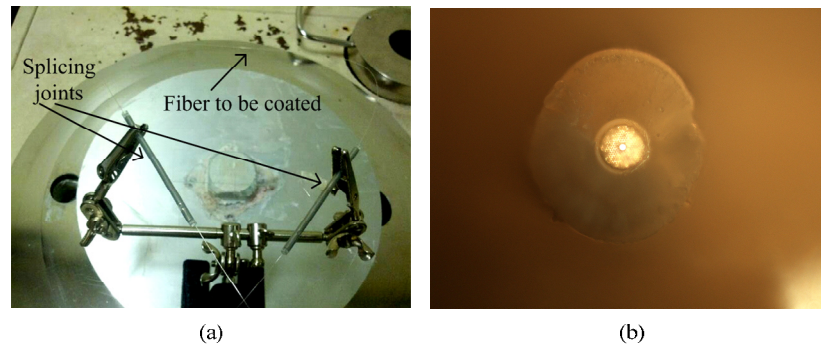


Fig. 2. (a) Coating configuration showing the fixture of fiber within the deposition chamber; (b) cross-section of a Parylene C coated HC-PBF. The diameter of the microstructured inner cladding is 70  $\mu\text{m}$ . The diameter of the outer silica cladding is 84  $\mu\text{m}$  (thickness:  $\sim 7$   $\mu\text{m}$ ), and it is coated with Parylene C to a jacket diameter of 284  $\mu\text{m}$ .

### 3 Measurement of acoustic response

Figure 3 shows the experimental setup for testing the acoustic response of the HC-PBF samples. The setup is a fiber-optic Michelson interferometer comprising a 2x2 directional coupler and two Faraday rotating mirrors (FRMs). The FRMs are used for polarization-fading mitigation [15]. The HC-PBF sample, with one end spliced to the coupler and the other end to the pigtail of the FRM, forms the sensing arm. The reference arm is made entirely from SMF. A single wavelength laser with its frequency modulated is used as the light source and the output from the interferometer is detected by a photo-detector and demodulated by a phase generated carrier (PGC) demodulation system [16, 17].

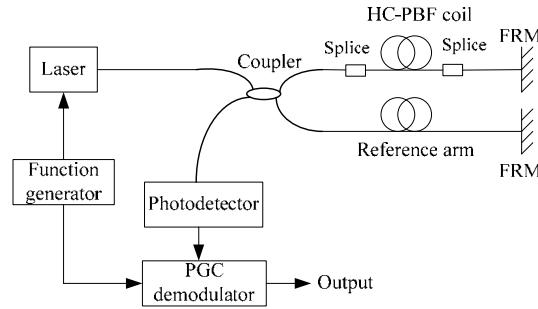


Fig. 3. Experimental setup

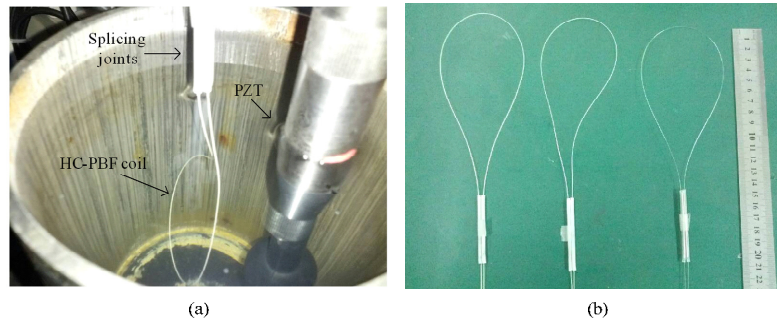


Fig. 4. (a) The acoustic test chamber filled with water; (b) three samples of HC-PBF sensing coils.

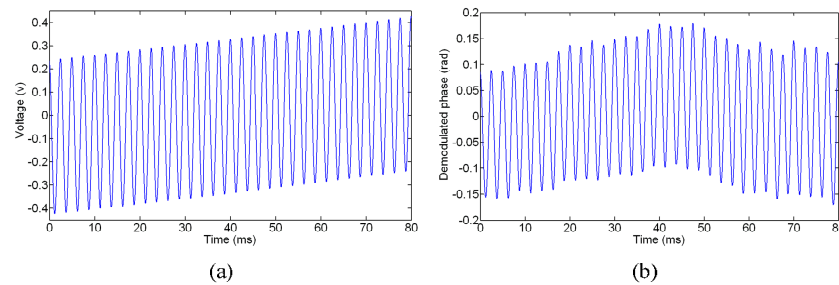


Fig. 5. Output from (a) the PZT transducer and (b) the fiber interferometer, when an acoustic signal at 400 Hz is applied.

The HC-PBF samples are coiled to a diameter of  $\sim 11$  cm (Fig. 4(b)) and put inside an acoustic testing chamber filled with water (Fig. 4(a)). The entire HC-PBF sample is submerged in water but the HC-PBF/SMF splicing joints and SMF pigtailed are above the water surface. A PZT transducer was put at the center of the HC-PBF coil and served as a calibrator. Figures 5(a) and 5(b) show respectively the output waveforms from the PZT calibrator and the fiber interferometer (after the PGC demodulator) for a HC-PBF sample with outer silica cladding thickness of  $7\text{ }\mu\text{m}$  and coated with Parylene C to a diameter of  $\sim 284\text{ }\mu\text{m}$ . The frequency of the applied acoustic signal is 400 Hz.

Figure 6 shows the frequency responses of four HC-PBF samples with the same length of 37 cm. The tests were carried out with the same setup and under the same experimental conditions. The mean responsivity, which is calculated by averaging the values from 250 to 2000 Hz, is shown in Table 1. The NRs of the samples are also shown in the Table 1. The responsivity of the sample with  $7\text{ }\mu\text{m}$ -thick outer silica cladding and  $100\text{ }\mu\text{m}$ -thick Parylene coating (Sample 3) is  $-183.94\text{ dB re rad}/\mu\text{Pa}$  or  $-313.46\text{ dB re }\mu\text{Pa}^{-1}$  in terms of NR. This

value is  $\sim 10$  dB higher than the HC-1550-02 fiber (Sample 2). Since the NR of HC-1550-02 fiber is shown to be  $\sim 15$  dB higher than a conventional SMF [11], the NR of the coated fiber (Sample 3) is estimated to be  $\sim 25$  dB higher than the conventional SMF.

It should be pointed out that the NR of the HC-1550-02 fiber (Sample 2) obtained here is larger than the theoretical value of  $-331.45$  dB re  $\mu\text{Pa}^{-1}$ . This could be partly caused by the acoustic response of the pigtail SMFs. Because the length of the sensing HC-PBFs is relatively short ( $\sim 37$  cm for all four samples) and the contribution of the SMF pigtails that are also exposed to the acoustic wave may not be neglected. However, since the four short samples were tested under similar conditions, the difference between NRs of different HC-PBF samples should be much less affected by the SMF pigtails.

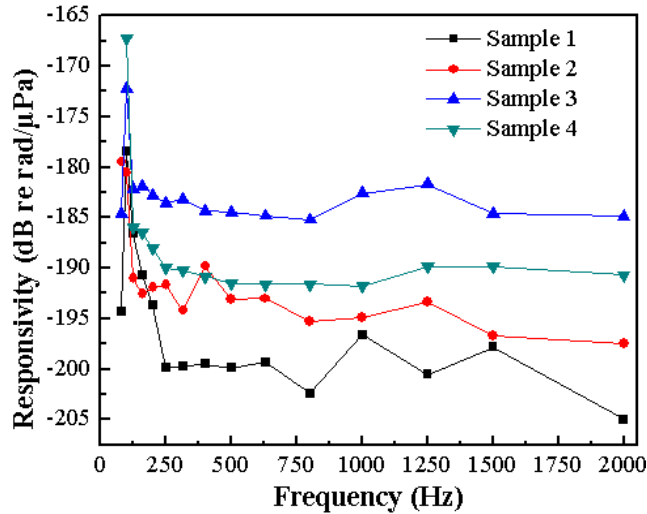


Fig. 6. Measured acoustic responsivity of four different HC-PBF samples. Sample 1: HC-1550-02 fiber without coating. Sample 2: HC-1550-02 fiber with original coating. Sample 3: the thicknesses of the outer silica cladding and the Parylene C coating are respectively  $7 \mu\text{m}$  and  $100 \mu\text{m}$ . Sample 4: the thicknesses of the outer silica cladding and the Parylene coating are respectively  $7 \mu\text{m}$  and  $22 \mu\text{m}$ .

Table 1. Mean responsivity between 250 and 2000Hz for four samples with a length of 37cm

Fiber Samples	Sample 1: HC-1550-02 fiber without coating	Sample 2: HC-1550-02 fiber with original coating	Sample 3: Etched HC-1550-02 fiber with $100 \mu\text{m}$ coating	Sample 4: Etched HC-1550-02 fiber with $22 \mu\text{m}$ coating
Mean Responsivity (dB re rad/ $\mu\text{Pa}$ )	-200.06	-193.95	-183.94	-190.78
NR (dB re $\mu\text{Pa}^{-1}$ )	-329.58	-323.47	-313.46	-320.30

#### 4. Discussion

The acoustic sensitivity of the HC-PBF samples are calculated numerically by using the model described in [11]. The model has four regions as shown in Fig. 7: region 1 is an air core with radius of  $a$ , region 2 is an air-silica honeycomb cladding with radius of  $b$ , region 3 is the outer silica cladding with radius of  $c$ , region 4 is a Parylene C polymer region with radius of  $d$ . The air-silica inner cladding is not a homogeneous material but behaves

mechanically like a honeycomb [18–20]. The Young's modulus and Poisson's ratio of this honeycomb cladding are the function of its air-filling ratio and can be determined once the air-filling ratio is known. The parameters of the four HC-PBF samples used in the numerical modeling are summarized in Table 2.

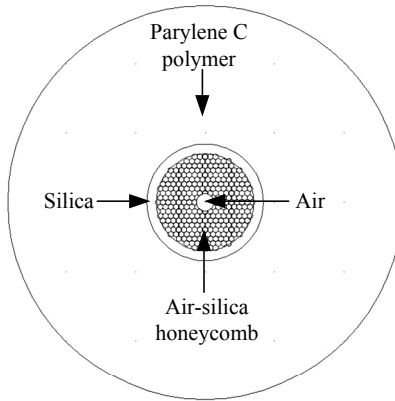


Fig. 7. Model of Sample 3 HC-PBF for mechanical analysis

Table 2. Physical parameters of the four HC-PBF samples

Fiber Samples	Sample 1	Sample 2	Sample 3	Sample 4
Region 1	Air $a = 5.45 \mu\text{m}$	Air $a = 5.45 \mu\text{m}$	Air $a = 5.45 \mu\text{m}$	Air $a = 5.45 \mu\text{m}$
Region 2	Air-silica honeycomb $b = 35 \mu\text{m}$ Air-filling ratio = 94%	Air-silica honeycomb $b = 35 \mu\text{m}$ Air-filling ratio = 94%	Air-silica honeycomb $b = 35 \mu\text{m}$ Air-filling ratio = 94%	Air-silica honeycomb $b = 35 \mu\text{m}$ Air-filling ratio = 94%
Region 3	Silica $c = 60 \mu\text{m}$ , $E_3 = 72$ GPa, $\nu_3 = 0.17$	Silica $c = 60 \mu\text{m}$ , $E_3 = 72$ GPa, $\nu_3 = 0.17$	Silica $c = 42 \mu\text{m}$ , $E_3 = 72 \text{ GPa}$ , $\nu_3 = 0.17$	Silica $c = 42 \mu\text{m}$ , $E_3 = 72 \text{ GPa}$ , $\nu_3 = 0.17$
Region 4	Air	Acrylate $d = 110 \mu\text{m}$ $E_4 = 0.5 \text{ GPa}$ , $\nu_4 = 0.37$	Parylene C $d = 142 \mu\text{m}$ $E_4 = 2.758 \text{ GPa}^*$ , $\nu_4 = 0.4^*$	Parylene C $d = 64 \mu\text{m}$ $E_4 = 2.758 \text{ GPa}^*$ , $\nu_4 = 0.4^*$

\* Data from Specialty Coating System for vacuum pressure of 25 mTorr within the deposition chamber [13, 14]

The calculated enhancement factors of the acoustic sensitivity of Sample 1, 3 and 4, relative to the original HC-1550-02 fiber (Sample 2) are shown in Table 3. The calculated and experimentally measured enhancement factors agree very well for Sample 1. This is expected since the Young's modulus and Poisson's ratio of the air-silica honeycomb and the silica outer cladding are determined accurately from the established data [11]. However, the theoretical results deviate significantly from the experimental data for Sample 3 and 4. This is also expected since the Young's modulus and Poisson's ratio of the Parylene C used for calculation are based on the value for 25 mTorr vacuum pressure within the deposition chamber [13]. Under this pressure, the deposition rate is very low ( $\sim 2 \mu\text{m}/\text{hour}$ ) and hence we have used a higher deposition pressure of  $\sim 100 \text{ mTorr}$ . This gives a much higher deposition rate of  $\sim 45 \mu\text{m}/\text{hour}$  but the density of the polymer coating is expected to be much smaller than for the 25 mTorr [21]. For the same polymer material, the Young's modulus decreases with reduction in density [22, 23], the Young's modulus of the Parylene C coating on the HC-PBFs is expected to be smaller than the value used in Table 2.

**Table 3. Enhancement factors of Sample 1, 3 and 4 relative to HC-1550-02 fiber (Sample 2)**

Fiber samples	Sample 1	Sample 3	Sample 4
Theoretical (dB)	−5.92	+ 5.70 ( $E_4 = 2.758$ GPa)	+ 1.84 ( $E_4 = 2.758$ GPa)
		+ 10.01 ( $E_4 = 0.798$ GPa)	+ 2.97 ( $E_4 = 0.798$ GPa)
Experimental (dB)	−6.11	+ 10.01	+ 3.17

We numerically calculated the sensitivity enhancement over the original HC-1550-02 fiber for varying Young's modulus of the polymer jacket and the result for Sample 3 is shown in Fig. 8. It can be seen that the value of Young's modulus of the polymer coating that matches the measured enhancement of 10.01 dB for Sample 3 is 0.798 GPa. With this value, the calculated enhancement of sensitivity for Sample 4 also approximately matches to its measured value (see Table 3), indicating the Young's modulus of the Parylene C coating is probably  $\sim 0.8$  GPa.

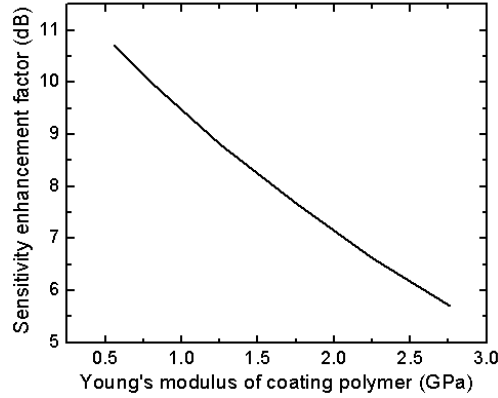


Fig. 8. Sensitivity enhancement factor of Sample 3 over the HC-1550-02 fiber (Sample 2) for varying Young's modulus of the polymer coating.

Figure 9 shows the numerically calculated radial displacement distribution for the commercial HC-1550-02 fiber (Sample 2) and a post-processed HC-1550-02 fiber (Sample 3), when a pressure of 1 kPa is applied to the fiber. The radial displacement distribution reflects the relative rigidity of different regions. The Young's modulus and Poisson's ratio of the polymer coating for Sample 3 were taken as for 0.795 GPa and 0.4, respectively. It shows the air-silica cladding region and polymer coating region are more flexible than the solid-silica outer cladding region. It is not difficult to understand that a fiber with less incompressible silica area would result in a larger axial strain under the same pressure. There is much less silica region in the post-processed HC-1550-02 fiber (Sample 3) as compared with original HC-1550-02 fiber (Sample 2), and hence the pressure sensitivity is significantly higher.

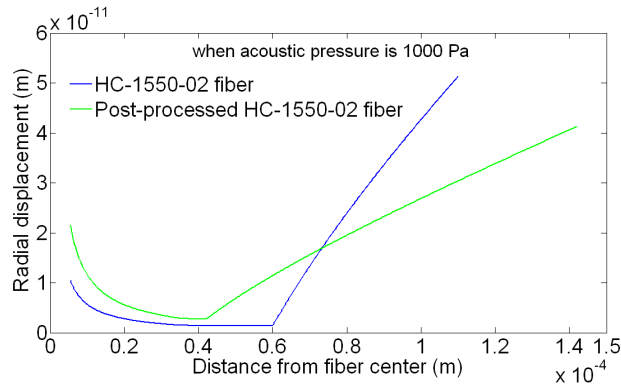


Fig. 9. Calculated radial displacement for the HC-PBF Samples 2 and 3.

## 5. Conclusion

We have experimentally demonstrated 10 dB improvement of the acoustic sensitivity by reducing the thickness of the silica outer cladding of the HC-1550-02 fiber down to 7  $\mu\text{m}$  and re-coating it with a Parylene C jacket. The achieved acoustic sensitivity is 25 dB higher than a conventional SMF, indicating significant improvement of acoustic sensitivity that could be achieved by optimizing the design of the HC-PBF. The samples used here are prepared by an etching and re-coating process and have relatively short length. However, a longer length of such fibers could readily be produced by a standard drawing process. The acoustic sensitivity could be further enhanced by optimizing the microstructured cladding and the polymer coating. The use of HC-PBF instead of conventional SMF would allow thinner coating to achieve a similar acoustic responsivity. The great improvement of acoustic responsivity is anticipated to have important practical benefits to simplify the sensor design of the fiber-optic hydrophone arrays, and increase the number of sensors that can be multiplexed in a single fiber. HC-PBFs can be bent down to very small diameters ( $< 1\text{ cm}$ ) with minimal loss, and are ideally suited for small-size hydrophone applications.

## Acknowledgments

This work was supported by the Hong Kong Special Administrative Region Government through a GRF grant PolyU5196/09E.